Number 61 | June 2023

SWISS NEUTRON NEWS

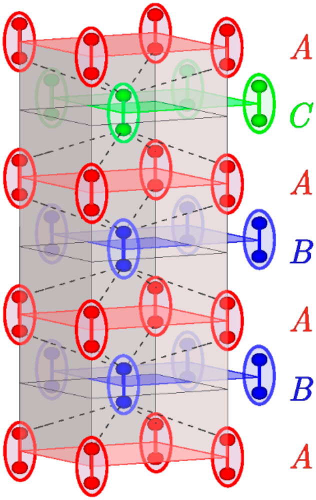

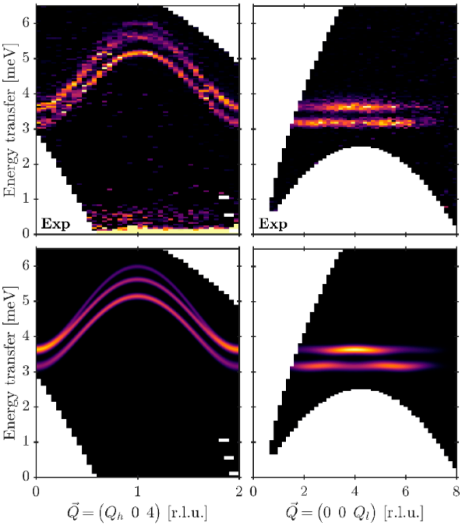

Schweizerische Gesellschaft für Neutronenforschung
Société Suisse de la Science Neutronique
Swiss Neutron Science Society

On the cover

(left) Illustration of a Terracotta Warrior that has been painted, among other ancient pigments, with the quantum magnetic compound Han Purple (©National Geographic).
(middle) Representation of the spin Hamiltonian of Han Purple containing three magnetic bilayer types arranged on six bilayers.
(right) Inelastic neutron scattering spectrum (experimental in top row and calculated in bottom row) along two high-symmetry directions in Q-space that has been essential for the determination of the spin Hamiltonian depicted in the middle.
Middle and right illustrations by S. Allenspach.

Contents

The President's Page

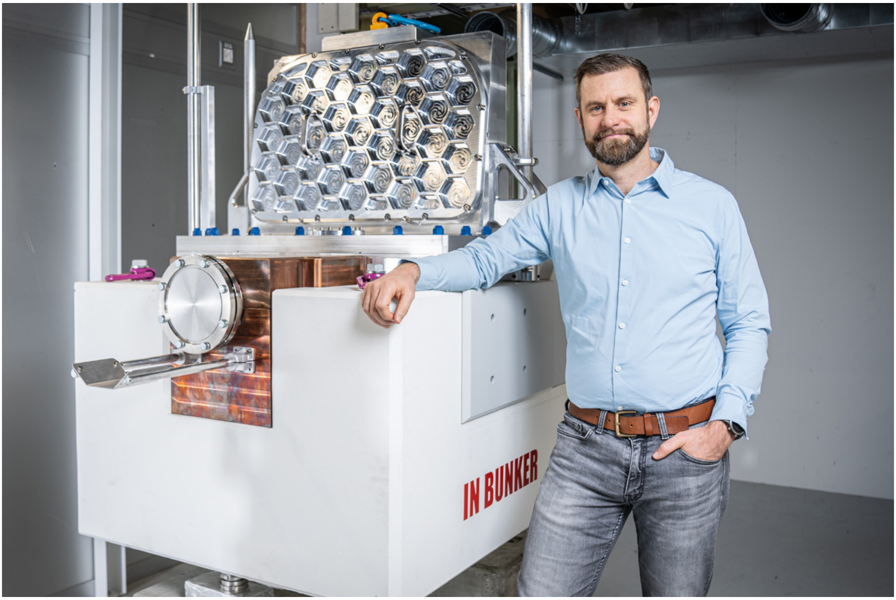

Dear fellow neutron scientists,

During our last general assembly on December 2, 2022, we decided that the Swiss Neutron Science Society should apply to become a member society of the Mathematic, Astronomy and Physics (MAP) platform of the Swiss Academy of Sciences (SCNAT). This decision was taken because this step will substantially increase the visibility of and opportunities for our society. Notably, being part of SCNAT results in synergies with other member societies that have common goals and interests (such as CHIPP, SPS, SGK/SSCr), for example, for the national roadmap process. We will also be able apply for funding from SCNAT to promote our society via activities such as summer schools/workshops, travel funds for members, and educational measures. In February, I submitted a formal application to SCNAT providing our motivation to join the MAP platform. I am glad to report that during the last meeting of the SCNAT executive board on March 31, 2023, this request was approved. The formal step took place at the SCNAT General Assembly on 26 May (https://scnat.ch/en/id/tMqqs?embed=ppsgG) and all of you are invited to join this event.

Apart from this important news, I would also like to express my thanks to Viviane Lutz-Bueno from the Paul Scherrer Institute who volunteered to take on the job of editing the Swiss Neutron News. Please join me in thanking her and her predecessor Efthymios Polatidis. You will find a short bio of Viviane after this editorial.

Otherwise, the year 2023 started with a highlight for European neutron scientists as from March 20-23, we all came together at the European Conference on Neutron Scattering in Garching, Germany. From my personal perspective, it was great to not only see so many of our old colleagues and collaborators at ECNS but also a new generation of neutron scientists starting out with their PhD and postdoc projects either using neutron instrumentation for their research or working on new instrumentation to push the boundaries of what is possible. From the Swiss perspective, it was also nice to see many Swiss colleagues and contributions to the meeting.

Talking about Swiss contributions, you will find two interesting articles describing recent successes of our community in this issue of Swiss Neutron News. They report on **exciting insights into quantum phase transitions (Stephan Allenspach, winner of last year's SNSS Young Scientist price)** and **on the design of capsules with surfactants, and the use of small angle scattering for their structural characterization**. With this I would also like to highlight that together with our Austrian colleagues the section Physics with Neutron and Synchrotron Radiation (NESY) within the Austrian Physical Society, we will again host a session on 'Neutron Science' at the Annual Meeting of the Swiss Physical Society that will take place from September 4-7, 2023 in Basel.

I wish all of you an exciting year and hope to meet you in Basel!

Marc Janoschek

New editor of Swiss Neutron News

Viviane Lutz-Bueno

Viviane Lutz-Bueno works on the field of small-angle scattering, with a particular focus on characterizing the structure of soft matter systems. As co-responsible for the commissioning and user program of the SANS-LLB instrument at SINQ, as well as being a lecturer at ETH Zurich, she has demonstrated her expertise in performing and interpreting standard and novel *in situ* SANS measurements, such as the structural mapping of fluids under flow.

Viviane's research interests span a broad spectrum, ranging from hierarchical biomaterials to self-assembled systems and alternative routes for biopolymers to material characterization. Her Ph.D. in soft matter physics from ETH Zurich, which she obtained in 2016, focused on exploring the structure-flow relationship of self-assembled micellar aggregates in microfluidic flows. Viviane utilized cutting-edge imaging techniques, such as flow-birefringence and scanning-SAXS, to gain insights into these systems.

As a postdoc at the Swiss Light Source, Viviane supported the user program of the cSAXS beamline, and continued to expand her expertise in material characterization, investigating and developing tensor tomography and scanning-SAXS techniques for use in the characterization of synthetic, composite, and biomaterials.

Quantum Criticality and Dimensionality in Quasi-2D Spin-Dimer Systems

S. Allenspach
Quantum Criticality and Dynamics Group,
Paul Scherrer Institute, CH-5232 Villigen-PSI,
Switzerland.*
Department of Quantum Matter Physics, University of Geneva, CH-1211 Geneva,
Switzerland.* and
Department of Chemistry and Applied
Biosciences, ETH Zurich, CH-8093 Zurich,
Switzerland.†

* Affiliations during PhD
† Current affiliation

Quantum phase transitions and critical phenomena can be investigated using spin-dimer systems that have been realized in various quantum magnetic compounds. Some quasi-low dimensional spin-dimer systems, which contain substructures that are strongly coupled internally and weakly to each other, display hallmarks of low-dimensional physics. Such systems allow the study of exotic physics in quantum magnetic compounds and might become relevant for future quantum engineering applications. We will discuss the search for hallmarks of two-dimensional physics in the layered spin-dimer systems $BaCuSi_2O_6$ and $Ba_{0.9}Sr_{0.1}CuSi_2O_6$. This article is based on my PhD thesis (Ref. [1]).

I. Introduction

Phase transitions can be encountered everywhere in nature from the melting of ice to the evolution of our universe from a primordial plasma to the cosmic structures observable today [2]. One of the basic concepts of statistical physics is that any continuous classical or quantum phase transition (QPT) can be assigned to a certain universality class that is specified by global and scale-invariant characteristics such as the dimensionality, symmetry, and in special cases also the topology [3].

Spin-dimer systems are ideal to study QPTs and have been realized in a vast number of compounds [4, 5]. In these systems, spin dimers, which consist of two spin-1/2 ions coupled via an antiferromagnetic (AF) and isotropic intra-dimer interaction, interact with each other via inter-dimer interactions. Due to the AF nature of the intra-dimer interactions, the ground state at zero temperature of these spin-dimer systems corresponds to a non-magnetic quantum paramagnetic state where all spin dimers are in their (non-magnetic) singlet state. The magnetic excitations are triplon quasiparticles, which correspond to triplet states that propagate over the spin-dimer lattice. Thus the dispersion contains three (one for each triplet state) degenerate and gapped triplon bands. When applying an external magnetic field, spin-dimer systems undergo a QPT at a critical field $\mu_0 H_{c1}$ to a phase whose ground state is a superposition of singlet and triplet (+) states that can be mapped to the XY-model [5–7].

If there is a hierarchy of inter-dimer interactions along different spatial directions, spin-dimer systems can contain one-dimensional (1D) or two-dimensional (2D) sub-structures, which are strongly coupled internally and weakly coupled to each other, and are called quasi-low dimensional. Examples for quasi-low dimensional spin-dimer systems have been identified in quasi-1D alternating spin chains, quasi-1D spin ladders, and quasi-2D layered compounds [1]. At zero temperature, the field induced ordered phase in spin-dimer systems is expected to be 3D XY, which resembles a Bose-Einstein Condensate [8, 9]. At finite temperatures the correlations between the low-dimensional substructures might become suppressed by temperature fluctuations thereby isolating these substructures leading to effectively low-dimensional physics.

In quasi-1D spin-dimer systems, a classical transition has been observed [10–13] to a quasi-1D Tomonaga-Luttinger Liquid phase with algebraically decaying spin-spin correlations [14, 15]. In quasi-2D spin-dimer system, a crossover has been proposed at a temperature T_{cr} from the low-temperature ordered phase into a quasi-2D phase with algebraically decaying spin-spin correlations [16]. This crossover has been suggested to be accompanied by a suppression of the magnetic order parameter above T_{cr} but has not been detected so far.

One question is “how 2D” a spin-dimer system has to be so that this conjectured suppression of the order parameter could be detected experimentally. Another question is if other hallmarks of 2D physics can be observed in quasi-2D spin-dimer systems. A major part of this article will therefore revolve around the dimensional reduction from 3D to 2D that has been proposed for the quasi-2D spin-dimer system $BaCuSi_2O_6$ [17].

II. $BaCuSi_2O_6$

$BaCuSi_2O_6$ is an ancient pigment, known as Han Purple, and was for example used to paint the famous Terracotta Army [18, 19]. At room temperature, its crystal structure is tetragonal and consists of bilayers hosting Cu^{2+}

spin-dimers that reside on a square lattice, while the squares on adjacent bilayers are relatively shifted by half their diagonal [20, 21]. This room temperature structure undergoes a first order structural phase transitions to a slightly orthorhombic low-temperature structure at 91(1) K (on cooling) shown in Fig. 1(a) [22–25].

Because the phase boundary of spin-dimer systems follows a power law in the critical regime close to the QCP at the critical field $\mu_0 H_{c1}$[27]

$$T_c(H) = \alpha(\mu_0 H - \mu_0 H_{c1})^{\phi},$$

where α is a non-universal scale parameter, the critical exponent $\phi = 2/d$ can be used to determine the dimensionality, d, of the field-induced XY-model. To extract ϕ of $BaCuSi_2O_6$, magnetic torque measurements were performed in the critical regime of this compound uncovering a shift from $\phi = 2/3$ (3D) to $\phi = 1$ (2D) when approaching the QCP. This shift has been confirmed by nuclear magnetic resonance (NMR) measurements [28] and was interpreted as dimensional reduction by Ref. [17].

Inelastic neutron scattering (INS) measurements performed at zero magnetic field observed multiple triplon modes [29] that can be explained by the presence of multiple dimer types. This explanation is supported by NMR measurements that reported two spectral lines [28, 30]. A detailed powder diffraction study [25] refined the average low-temperature crystal structure and revealed that adjacent bilayers differ structurally [Fig. 1(a)] thereby resulting in at least two types of bilayers that might host different dimer types.

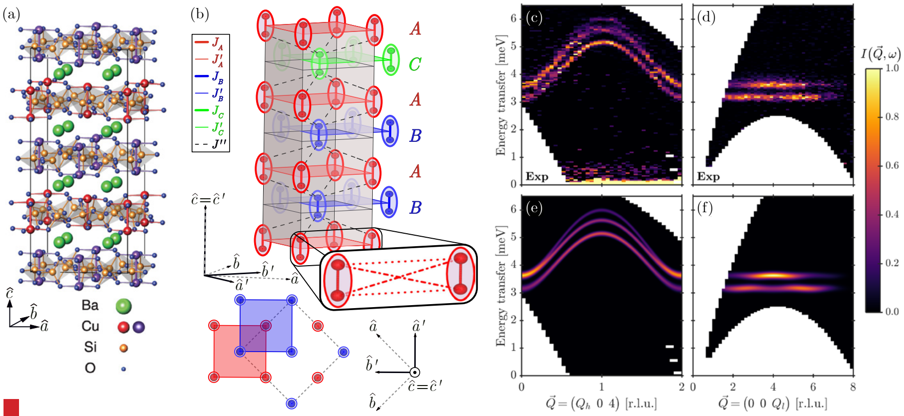

Figure 1

INS investigation of $BaCuSi_2O_6$. (a) Low-temperature crystal structure of $BaCuSi_2O_6$ containing two types of structurally inequivalent bilayers indicated by the two Cu-ion colors. (b) Magnetic model determined for this compound with three bilayer types arranged on six bilayers. (d, e) INS spectra measured for $BaCuSi_2O_6$ on AMATERAS at 0.3~K and at zero magnetic field along two high-symmetry directions. Data was collected in the experimental unit cell $(\vec{a}, \vec{b}, \vec{c})$ illustrated in panel (b). (f, g) Calculated spectrum using the model displayed in panel (b). Panels (a) and (b-g) are adapted from Ref. [25] and Ref. [26], respectively.

The aforementioned dimensional reduction is highly unconventional, because the opposite behavior – namely a dimensional crossover from 2D to 3D – would be expected in the critical regime when approaching the QPT due to a diverging correlation length. Thus a plethora of theories were formulated to explain this dimensional reduction. Most of these theories assume AF intra-bilayer interactions, based on [29, 31, 32] resulting in geometrical frustration of the inter-bilayer interaction as proposed in Ref. [17]. Some theories involve only one bilayer type and rely on perfect frustration [33–35] but were contested by Refs. [36–38]. Others include two bilayer types with either perfect or imperfect frustration and explain the dimensional reduction as cooperative effect of frustration and an energy mismatch of the inequivalent bilayers [38–40]. An *ab initio* study [41] proposed effectively ferromagnetic (FM) intra-bilayer interactions in $BaCuSi_2O_6$ that would render the frustration of the inter-bilayer interaction impossible thereby making most of the aforementioned theories inapplicable to this compound.

To answer the question of the sign of the intra-bilayer interactions in $BaCuSi_2O_6$, we have performed zero field high-resolution INS measurements on the time-of-flight spectrometers AMATERAS at J-PARC [42] and LET at ISIS [43] using temperatures of 0.3 K and 1.6 K, respectively [26]. The triple-axis spectrometers (TAS) EIGER [44] and TASP [45] both at the SINQ neutron source were used for further investigation of selected $\vec{Q}$ directions, measuring at 1.6 K on both. All experiments used one flux-grown single crystal of $BaCuSi_2O_6$ with a mass of 1.01 g. Figure 1(c, d) displays the INS spectrum of BaCuSi2O6 collected on AMATERAS along two high-symmetry directions. At least three triplon modes – labeled A, B, and C from lowest to highest energy – could be resolved in our data in agreement with Ref. [29].

To model the INS spectrum of $BaCuSi_2O_6$, we generalized the method of Refs. [46, 47] to multiple dimer types [26]. We assume that the only magnetic interactions are those shown in Fig. 1(b) and that they have purely Heisenberg character. A comparison of the mode intensities along (1 0 Q_l), allowed the determination of the dimer types ratio A:B:C ≈ 3:2:1 [26]. Assuming that one structural bilayer type hosts only one dimer type, this ratio suggests a magnetic unit cell containing an ABABAC bilayer stacking.

A fit of our model [Fig. 1(b)] to the INS data (as described in Ref. [26]) yields the intra-dimer interaction parameters $J_A = 4.275(5)$ meV, $J_B = 4.72(1)$ meV, and $J_C = 4.95(2)$ meV, intra-bilayer interactions $J'_A = -0.480(3)$ meV, $J'_B = -0.497(8)$ meV, and $J'_C = -0.57(1)$ meV, and the inter-bilayer interaction $J'' = -0.04(1)$ meV, where $J < 0$ refers to FM interactions [26]. These optimal values were used to calculate the INS spectrum shown in Fig. 1(e, f). The intra-bilayer interactions (J'_A , J'_B , and J'_C) are effectively FM as proposed by Ref. [41] thereby rendering frustration of the inter-bilayer interaction impossible in $BaCuSi_2O_6$. Thus the crucial questions are first how the shift in the critical exponent, ϕ, from 2/3 (3D) to 1 (2D) observed in $BaCuSi_2O_6$ [17] can be explained without this frustration, and second, if the bilayer stacking plays an essential part or not. To answer these questions, our collaborators performed Quantum Monte Carlo (QMC) simulations [48] of the six-bilayer (ABABAC) model shown in Fig. 1(b) using the determined interaction parameters at zero field. With the help of these QMC simulations, it was possible to deduce that thermal fluctuations suppress the tunneling between the A bilayers so that they become decoupled for temperatures above $(J'')^2/(J_A - J_B)$, which corresponds approximately to 40 mK, resulting in an anomalous scaling regime [26] originally observed and interpreted as dimensional reduction by Ref. [17].

Although $BaCuSi_2O_6$ displays 3D physics at the QPT [26], the question remains if hallmarks of 2D physics might be observable at higher temperatures (similar to the ones proposed by Ref. [16]) due to the aforementioned bilayer energy mismatch. For example, one could imagine that the order parameter remain strongly suppressed over the regime $H_{c1} < H < H^*$, where $H^* - H_{c1} = (J_B - J_A)/g\mu_B\mu_0$, until the field establishes a significant triplon occupation on all bilayers [49].

To investigate if the magnetic order parameter deviates from a conventional form (i.e. due to the aforementioned suppression), we have performed neutron scattering experiments at magnetic fields up to 25.9 T using the High Field Magnet system [50] in combination with the Extreme Environment Diffractometer instrument [51–53] at the Helmholtz-Zentrum in Berlin [49]. These experiments were conducted with the same single crystal of $BaCuSi_2O_6$ used already for the aforementioned INS measurements. We measured the nuclear and magnetic intensities of the (−2 0 2) Bragg peak for various combinations of magnetic fields and temperatures within and outside the field-induced phase. A model of the Bragg peak intensity has been constructed under the assumption of a conventional form of the magnetic order parameter. The posterior distribution of the model parameters conditional on the measured Bragg peak intensities has been determined using Bayesian inference [49]. As the posterior distribution of the model agrees well with the data, we conclude that the order parameter is not suppressed within the measured field and temperature range.

III. Ba0.9Sr0.1CuSi2O6

The inequivalent bilayers of the low-temperature structure in $BaCuSi_2O_6$ appear to complicate the physics of an otherwise ideal model system to study criticality in quasi-2D spin-dimer compounds. Stoichiometric substitution of Sr ions on the Ba sites was used to generate $Ba_{0.9}Sr_{0.1}CuSi_2O_6$ [54] whose tetragonal crystal structure, shown in Fig. 2(a), persists down to 1.5 K [55].

To determine the dimer interaction parameters and verify the presence of only a single bilayer type in $Ba_{0.9}Sr_{0.1}CuSi_2O_6$ [56], we have performed INS measurements at 1.5 K and at zero magnetic field on TASP [45] as well as on the novel multiplexing TAS instrument CAMEA [57] both at the SINQ neutron source. A rodshaped single crystal of $Ba_{0.9}Sr_{0.1}CuSi_2O_6$ with a mass of 1.3 g (characterized in Ref. [58]) was used for these measurements.

Data collected on CAMEA has been preprocessed using the software MJOLNIR [59]. The spectrum measured on CAMEA is displayed in Fig. 2(c, d) along two high-symmetry directions. In comparison to the INS spectrum of $BaCuSi_2O_6$, for which at least three triplon modes can be resolved [Fig. 1(c, d)], only one triplon mode is visible in the INS spectrum of $Ba_{0.9}Sr_{0.1}CuSi_2O_6$ confirming the

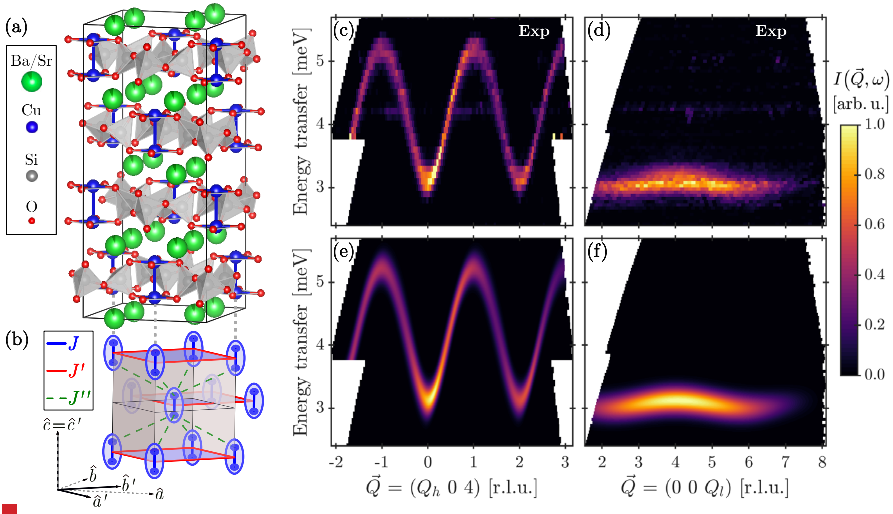

Figure 2
INS investigation of $Ba_{0.9}Sr_{0.1}CuSi_2O_6$. (a) Crystal structure of $Ba_{0.9}Sr_{0.1}CuSi_2O_6$ containing only one bilayer type [55]. (b) Magnetic model determined for this compound with one bilayer type arranged on two bilayers. (d, e) INS spectra measured for $Ba_{0.9}Sr_{0.1}CuSi_2O_6$ on CAMEA at 1.5~K and at zero magnetic field along two high-symmetry directions. Data was collected in the experimental unit cell $(\vec{a}, \vec{b}, \vec{c})$ illustrated in panel (b). (f, g) Calculated spectrum using the model displayed in (b). The figure is adapted from Ref. [56].

presence of only one dimer type in this compound. Thus a magnetic model with equivalent bilayers has been constructed and is shown in Fig. 2(b). This model has been fitted to the INS data (as described in Ref. [56]) resulting in $J = 4.28(2)$, $J' = -0.52(1)$, and $J''= -0.02(1)$ [56]. These optimal values were used to calculate the INS spectrum shown in Fig. 2(e, f). We note that the intra-bilayer interaction is also effectively FM as for $BaCuSi_2O_6$.

Because the presence of multiple bilayers has been causing the anomalous scaling regime in $BaCuSi_2O_6$, the question arises whether the critical exponent, ϕ, of $Ba_{0.9}Sr_{0.1}CuSi_2O_6$ agrees with the conventional value (2/3) of the 3D XY universality class as expected or not. To answer this question, our collaborators have performed ^{29}Si NMR spectroscopy measurements using a 13 mg single crystal of $Ba_{0.9}Sr_{0.1}CuSi_2O_6$ obtaining NMR spectra at 10 different temperatures ranging from 49 up to 921 mK [56]. The magnetic order parameter of spin-dimer systems is proportional to the line splitting in NMR spectra [60]. Thus its field dependence could be determined for each of these 10 NMR spectra, which was then used to extract the phase boundary of $Ba_{0.9}Sr_{0.1}CuSi_2O_6$ close to the QCP [56]. These points have been analyzed using Bayesian inference to determine the joint posterior distribution of the phase boundary model parameters in Eq. (1) [56]. The extent of the critical regime, in which the phase boundary model is applicable, is non-universal and *a priori* unknown. Thus, the analysis was repeated for different subsets, where for each subset only points up to a maximal temperature were included in the analysis. We found that ϕ has a clear tendency to 2/3 as expected for 3D XY [56].

$Ba_{0.9}Sr_{0.1}CuSi_2O_6$ can be considered an ideal quasi-2D spin-dimer systems with only one dimer type and $J'/J'' \approx 25$. The question arises if a suppression of the magnetic order parameter as conjectured by Ref. [16], might be observable in this compound. As the conventional form for the order parameter is in good agreement with the NMR line splitting, we conclude that the order parameter is not suppressed within the measured field and temperature range in $Ba_{0.9}Sr_{0.1}CuSi_2O_6$.

IV. Conclusion

We have presented our search for hallmarks of 2D physics in the layered spin-dimer compounds $BaCuSi_2O_6$ and $Ba_{0.9}Sr_{0.1}CuSi_2O_6$. For $BaCuSi_2O_6$ we found a magnetic model with three bilayer types, arranged in an ABABAC stacking, and effectively FM intra-bilayer interactions within all bilayer types. Thus, frustration of the inter-bilayer interactions is impossible making most explanations of the shift in ϕ from 3D to 2D, observed in Ref. [17], inapplicable. QMC simulations based on the determined magnetic model of $BaCuSi_2O_6$ reveal an anomalous scaling regime caused by the multi-bilayer structure and therefore provide a quantitative explanation of the observed shift in ϕ that was originally misinterpreted as dimensional reduction.

Neutron diffraction experiments at magnetic fields up to 25.9 T were used to extract the field and temperature dependence of the (−2 0 2) Bragg peak intensity in $BaCuSi_2O_6$. No suppression of the order parameter, either as conjectured by Ref. [16] for quasi-2D spin-dimer systems or imaginable for $BaCuSi_2O_6$ due to the energy mismatch between its adjacent bilayers, could be detected in our data.

For $Ba_{0.9}Sr_{0.1}CuSi_2O_6$ we found a magnetic Hamiltonian with only one spin-dimer type as proposed by Ref. [55] and effectively FM intra-bilayer interaction parameters as in $BaCuSi_2O_6$. By analyzing the phase boundary extracted from NMR spectra, we verify that $Ba_{0.9}Sr_{0.1}CuSi_2O_6$ displays a critical exponent compatible with 3D XY without any signs of an anomalous scaling regime observed in $BaCuSi_2O_6$. Although $Ba_{0.9}Sr_{0.1}CuSi_2O_6$ is a quasi-2D spin-dimer system ($J'/J'' \approx 25$), we could not detect any evidence for a suppression of the order parameter, as conjectured by Ref. [16], in our data.

The search for hallmarks of 2D physics in quasi-2D spin-dimer systems continues. This search will require experiments at high magnetic fields that will be analyzed using modern statistical methods and interpreted with the help of computer simulations. Thus further development in the areas of instrumentation, sample environment, crystal growth, theory, high-performance computing, experimental design, and data analysis will be essential for the success of this search.

ACKNOWLEDGMENTS

I would like to thank Ch. Rüegg, B. Normand, N. Laflorencie, F. Mila, A. Madsen, A. Biffin, F. Giorgianni, S. Ward, S. Tóth, P. Puphal, O. K. Forslund, M. Månsson, P. Naumov, S. Nikitin,

D. Sheptyakov, M. Janoschek, R. Stern, and M. Horvatić for their guidance and helpful discussions concerning various aspects of the presented research. This research would not have been possible without the instrument scientists and technicians that supported me during my neutron scattering experiments: Ch. Kägi, J. Stahn, G. S. Tucker, U. Stuhr, D. J. Voneshen, M. Boehm, S. Ohira-Kawamura, M. Kofu, J. Lass, Ch. Nieder mayer, O. Prokhnenko, M. Bartkowiak, X. Liu, A. Gazizulina, P. Smeibidl, P. Heller, S. Kempfer, R. Wahle, and S. Gerischer. I am grateful to N. Laflorencie and F. Mila for the QMC simulations and to I. Fisher, S. Sebastian, P. Puphal, and E. Pomjakushina for sample growth. Moreover, I would like to thank the members of the $Ba_{0.9}Sr_{0.1}CuSi_2O_6$ collaboration that have not yet been mentioned: J. Link, I. Heinmaa, C. Krellner, S. Imajo, Y. Kohama, K. Kindo, S. Krämer, M. Jaime, A. Mira, F. Weickert. Lastly, my thank goes to the Swiss Neutron Science Society and G. Schneider for giving me the opportunity to present the content of my PhD thesis in this article.

[1] S. Allenspach, *Quantum Criticality and Dimensionality in Quasi-2D Spin-Dimer Systems*, Ph.D. thesis, University of Geneva (2021).

[2] E. W. Kolb, Cosmological Phase Transitions, in *Gravitation in Astrophysics: Cargèse 1986*, edited by B. Carter and J. B. Hartle (Springer US, Boston, MA, 1987) pp. 307–327.

[3] J. Zinn-Justin, *Quantum Field Theory and Critical Phenomena* (Oxford University Press, Oxford, 2002).

[4] M. Hase, Spin-Peierls transition in CuGeO3, Physica B: Condensed Matter **237-238**, 123 (1997).

[5] V. Zapf, M. Jaime, and C. D. Batista, Bose-Einstein condensation in quantum magnets, Rev. Mod. Phys. **86**, 563 (2014).

[6] M. Matsumoto, B. Normand, T. M. Rice, and M. Sigrist, Magnon Dispersion in the Field-Induced Magnetically Ordered Phase of $TlCuCl_3$, Phys. Rev. Lett. **89**, 077203 (2002).

[7] T. Giamarchi, C. Rüegg, and O. Tchernyshyov, Bose–Einstein condensation in magnetic insulators, Nat. Phys. **4**, 198 (2008).

[8] S. N. Bose, Plancks Gesetz und Lichtquantenhypothese, Z. Phys. **26**, 178 (1924).

[9] A. Einstein, Quantentheorie des einatomigen idealen Gases, Sitz. Ber. Kgl. Preuss. Akad. Wiss. **3**, 261 (1924).

[10] M. Klanjšek, H. Mayaffre, C. Berthier, M. Horvatić, B. Chiari, O. Piovesana, P. Bouillot, C. Kollath, E. Orignac, R. Citro, and T. Giamarchi, Controlling Luttinger Liquid Physics in Spin Ladders under a Magnetic Field, Phys. Rev. Lett. **101**, 137207 (2008).

[11] B. Thielemann, C. Rüegg, K. Kiefer, H. M. Rønnow, B. Normand, P. Bouillot, C. Kollath, E. Orignac, R. Citro, T. Giamarchi, A. M. Läuchli, D. Biner, K. W. Krämer, F. Wolff-Fabris, V. S. Zapf, M. Jaime, J. Stahn, N. B. Christensen, B. Grenier, D. F. McMorrow, and J. Mesot, Field-controlled magnetic order in the quantum spin-ladder system $(Hpip)_2\,CuBr_4$, Phys. Rev. B **79**, 020408 (2009).

[12] D. Schmidiger, P. Bouillot, S. Mühlbauer, S. Gvasaliya, C. Kollath, T. Giamarchi, and A. Zheludev, Spectral and Thermodynamic Properties of a Strong-Leg Quantum Spin Ladder, Phys. Rev. Lett. **108**, 167201 (2012).

[13] K. Ninios, T. Hong, T. Manabe, C. Hotta, S. N. Herringer, M. M. Turnbull, C. P. Landee, Y. Takano, and H. B. Chan, Wilson Ratio of a Tomonaga-Luttinger Liquid in a Spin-1/2 Heisenberg Ladder, Phys. Rev. Lett. **108**, 097201 (2012).

[14] S. Sachdev, Quantum phase transitions and conserved charges, Zeitschrift für Physik B Condensed Matter **94**, 469 (1994).

[15] T. Giamarchi and A. M. Tsvelik, Coupled ladders in a magnetic field, Phys. Rev. B **59**, 11398 (1999).

[16] S. C. Furuya, M. Dupont, S. Capponi, N. Laflorencie, and T. Giamarchi, Dimensional modulation of spontaneous magnetic order in quasi-two-dimensional quantum antiferromagnets, Phys. Rev. B. **94**, 144403 (2016).

[17] S. E. Sebastian, N. Harrison, C. D. Batista, L. Balicas, M. Jaime, P. A. Sharma, N. Kawashima, and I. R. Fisher, Dimensional reduction at a quantum critical point, Nature **441**, 617 (2006).

[18] E. W. FitzHugh and L. A. Zycherman, A Purple Barium Copper Silicate Pigment from Early China, Stud. Conserv. **37**, 145 (1992).

[19] M. Martinón-Torres, X. J. Li, A. Bevan, Y. Xia, K. Zhao, and T. Rehren, Forty Thousand Arms for a Single Emperor: From Chemical Data to the Labor Organization Behind the Bronze Arrows of the Terracotta Army, Journal of Archaeological Method and Theory **21**, 534 (2014).

[20] L. W. Finger, R. M. Hazen, and R. J. Hemley, $BaCuSi_2O_6$: A new cyclosilicate with four-membered tetrahedral rings, Am. Miner. **74**, 952 (1989).

[21] Y. Sasago, K. Uchinokura, A. Zheludev, and G. Shirane, Temperature-dependent spin gap and singlet ground state in $BaCuSi_2O_6$, Phys. Rev. B **55**, 8357 (1997).

[22] K. Sparta, M. Merz, G. Roth, R. Stern, R. Cerny, and T. Kimura, Low temperature phase transition in $BaCuSi_2O_6$, Acta Cryst. A **62**, S197 (2006).

[23] E. C. Samulon, Z. Islam, S. E. Sebastian, P. B. Brooks, M. K. McCourt, J. Ilavsky, and I. R. Fisher, Low-temperature structural phase transition and incommensurate lattice modulation in the spin-gap compound $BaCuSi_2O_6$, Phys. Rev. B **73**, 100407 (2006).

[24] R. Stern, I. Heinmaa, E. Joon, A. A. Tsirlin, H. Nakamura, and T. Kimura, Low-Temperature High-Resolution Solid-State (cryoMAS) NMR of Han Purple $BaCuSi_2O_6$, Appl. Magn. Reson. **45**, 1253 (2014).

[25] D. V. Sheptyakov, V. Y. Pomjakushin, R. Stern, I. Heinmaa, H. Nakamura, and T. Kimura, Two types of adjacent dimer layers in the low-temperature phase of $BaCuSi_2O_6$, Phys. Rev. B **86**, 014433 (2012).

[26] S. Allenspach, A. Biffin, U. Stuhr, G. S. Tucker, S. Ohira-Kawamura, M. Kofu, D. J. Voneshen, M. Boehm, B. Normand, N. Laflorencie, F. Mila, and C. Rüegg, Multiple Magnetic Bilayers and Unconventional Criticality without Frustration in $BaCuSi_2O_6$, Phys. Rev. Lett. **124**, 177205 (2020).

[27] N. Kawashima, Quantum Critical Point of the XY Model and Condensation of Field-Induced Quasiparticles in Dimer Compounds, J. Phys. Soc. Jpn. **73**, 3219 (2004).

[28] S. Krämer, R. Stern, M. Horvatić, C. Berthier, T. Kimura, and I. R. Fisher, Nuclear magnetic resonance evidence for a strong modulation of the Bose-Einstein condensate in $BaCuSi_2O_6$, Phys. Rev. B **76**, 100406 (2007).

[29] C. Rüegg, D. F. McMorrow, B. Normand, H. M. Rønnow, S. E. Sebastian, I. R. Fisher, C. D. Batista, S. N. Gvasaliya, C. Niedermayer, and J. Stahn, Multiple Magnon Modes and Consequences for the Bose-Einstein Condensed Phase in $BaCuSi_2O_6$, Phys. Rev. Lett. **98**, 017202 (2007).

[30] S. Krämer, N. Laflorencie, R. Stern, M. Horvatić, C. Berthier, H. Nakamura, T. Kimura, and F. Mila, Spatially resolved magnetization in the Bose-Einstein condensed state of $BaCuSi_2O_6$: Evidence for imperfect frustration, Phys. Rev. B **87**, 180405 (2013).

[31] M. Jaime, V. F. Correa, N. Harrison, C. D. Batista, N. Kawashima, Y. Kazuma, G. A. Jorge, R. Stern, I. Heinmaa, S. A. Zvyagin, Y. Sasago, and K. Uchinokura, Magnetic-Field-Induced Condensation of Triplons in Han Purple Pigment $BaCuSi_2O_6$, Phys. Rev. Lett. **93**, 087203 (2004).

[32] S. E. Sebastian, P. A. Sharma, M. Jaime, N. Harrison, V. Correa, L. Balicas, N. Kawashima, C. D. Batista, and I. R. Fisher, Characteristic Bose-Einstein condensation scaling close to a quantum critical point in $BaCuSi_2O_6$, Phys. Rev. B **72**, 100404 (2005).

[33] C. D. Batista, J. Schmalian, N. Kawashima, P. Sengupta, S. E. Sebastian, N. Harrison, M. Jaime, and I. R. Fisher, Geometric Frustration and Dimensional Reduction at a Quantum Critical Point, Phys. Rev. Lett. **98**, 257201 (2007).

[34] J. Schmalian and C. D. Batista, Emergent symmetry and dimensional reduction at a quantum critical point, Phys. Rev. B **77**, 094406 (2008).

[35] Y. Kamiya, N. Kawashima, and C. D. Batista, Finite-Temperature Transition in the Spin-Dimer Antiferromagnet $BaCuSi_22O_6$, J. Phys. Soc. Jpn. **78**, 094008 (2009).

[36] M. Maltseva and P. Coleman, Failure of geometric frustration to preserve a quasi-two-dimensional spin fluid, Phys. Rev. B **72**, 174415 (2005).

[37] O. Rösch and M. Vojta, Quantum phase transitions and dimensional reduction in antiferromagnets with inter-layer frustration, Phys. Rev. B **76**, 180401 (2007).

[38] O. Rösch and M. Vojta, Reduced dimensionality in layered quantum dimer magnets: Frustration vs. inhomogeneous condensates, Phys. Rev. B **76**, 224408 (2007).

[39] N. Laflorencie and F. Mila, Theory of the Field-Induced BEC in the Frustrated Spin-1/2 Dimer Compound $BaCuSi_2O_6$, Phys. Rev. Lett. **102**, 060602 (2009).

[40] N. Laflorencie and F. Mila, Condensate-Free Superfluid Induced by the Frustrated Proximity Effect, Phys. Rev. Lett. **107**, 037203 (2011).

[41] V. V. Mazurenko, M. V. Valentyuk, R. Stern, and A. A. Tsirlin, Nonfrustrated Interlayer Order and its Relevance to the Bose-Einstein Condensation of Magnons in $BaCuSi_2O_6$, Phys. Rev. Lett. **112**, 107202 (2014).

[42] K. Nakajima, S. Ohira-Kawamura, T. Kikuchi, M. Nakamura, R. Kajimoto, Y. Inamura, N. Takahashi, K. Aizawa, K. Suzuya, K. Shibata, T. Nakatani, K. Soyama, R. Maruyama, H. Tanaka, W. Kambara, T. Iwahashi, Y. Itoh, T. Osakabe, S. Wakimoto, and M. Arai, AMATERAS : A cold-neutron disk chopper spectrometer, J. Phys. Soc. Jpn. **80**, SB028 (2011).

[43] R. I. Bewley, J. W. Taylor, and S. M. Bennington., LET, a cold neutron multi-disk chopper spectrometer at ISIS, Nucl. Instrum. Methods A **637**, 128 (2011).

[44] U. Stuhr, B. Roessli, S. Gvasaliya, H. M. Rønnow, U. Filges, D. Graf, A. Bollhalder, D. Hohl, R. Bu¨ rge, M. Schild, L. Holitzner, C. K¨ agi, P. Keller, and T. Mühlebach, The thermal triple-axis-spectrometer EIGER at the continuous spallation source SINQ, Nucl. Instrum. Methods A **853**, 16 (2017).

[45] P. Böni and P. Keller, Polarized Triple Axis Spectrometer TASP, Proceedings of the 4th Summer School on Neutron Scattering **96**, 35 (1996).

[46] B. Leuenberger, H.-U. Güdel, R. Feile, and J. K. Kjems, Collective excitations in the singlet-ground-state dimer system $Cs_3Cr_2Br_9$, Phys. Rev. B **28**, 5368 (1983).

[47] B.Leuenberger, A.Stebler, H.U.Güdel, A.Furrer, R. Feile, and J. K. Kjems, Spin dynamics of an isotropic singlet-ground-state antiferromagnet with alternating strong and weak interactions: An inelastic-neutron-scattering study of the dimer compound $Cs_3Cr_2Br_9$, Phys. Rev. B **30**, 6300 (1984).

[48] O. F. Syljuåsen and A. W. Sandvik, Quantum Monte Carlo with directed loops, Phys. Rev. E **66**, 046701 (2002).

[49] S. Allenspach, A. Madsen, A. Biffin, M. Bartkowiak, O. Prokhnenko, A. Gazizulina, X. Liu, R. Wahle, S. Gerischer, S. Kempfer, P. Heller, P. Smeibidl, A. Mira, N. Laflorencie, F. Mila, B. Normand, and C. Rüegg, Investigating field-induced magnetic order in Han purple by neutron scattering up to 25.9 T, Phys. Rev. B **106**, 104418 (2022).

[50] P. Smeibidl, M. Bird, H. Ehmler, I. Dixon, J. Heinrich, M. Hoffmann, S. Kempfer, S. Bole, J. Toth, O. Prokhnenko, and B. Lake, First Hybrid Magnet for Neutron Scattering at Helmholtz-Zentrum Berlin, IEEE Transactions on Applied Superconductivity **26**, 1 (2016).

[51] M. Bartkowiak, N. Stüsser, and O. Prokhnenko, The design of the inelastic neutron scattering mode for the Extreme Environment Diffractometer with the 26T High Field Magnet, Nuclear Instruments and Methods in Physics Research Section A: Accelerators, Spectrometers, Detectors and Associated Equipment **797**, 121 (2015).

[52] O. Prokhnenko, W.-D. Stein, H.-J. Bleif, M. Fromme, M. Bartkowiak, and T. Wilpert, Time-of-flight Extreme Environment Diffractometer at the Helmholtz-Zentrum Berlin, Rev. Sci. Instr. **86**, 033102 (2015).

[53] O. Prokhnenko, P. Smeibidl, W.-D. Stein, M.Bartkowiak,andN.Stüsser,HFM/EXED:The High Magnetic Field Facility for Neutron Scattering at BER II, Journal of large-scale research facilities JLSRF **3** (2017), 10.17815/jlsrf-3-111.

[54] N. van Well, P. Puphal, B. Wehinger, M. Kubus, J. Schefer, C. Rüegg, F. Ritter, C. Krellner, and W. Assmus, Crystal Growth with Oxygen Partial Pressure of the $BaCuSi_2O_6$ and $Ba_{1-x}Sr_xCuSi_2O_6$ Spin Dimer Compounds, Cryst. Growth & Design **16**, 3416 (2016).

[55] P. Puphal, D. Sheptyakov, N. van Well, L. Postulka, I. Heinmaa, F. Ritter, W. Assmus, B. Wolf, M. Lang, H. O. Jeschke, R. Valentí, R. Stern, C. Rüegg, and C. Krellner, Stabilization of the tetragonal structure in $(Ba_{1-x}Sr_x)CuSi_2O_6$, Phys. Rev. B **93**, 174121 (2016).

[56] S. Allenspach, P. Puphal, J. Link, I. Heinmaa, E. Pomjakushina, C. Krellner, J. Lass, G. S. Tucker, C. Niedermayer, S. Imajo, Y. Kohama, K. Kindo, S. Krämer, M. Horvatić, M. Jaime, A. Madsen, A. Mira, N. Laflorencie, F. Mila, B. Normand, C. Rüegg, R. Stern, and F. Weickert, Revealing three-dimensional quantum criticality by Sr substitution in Han purple, Phys. Rev. Research **3**, 023177 (2021).

[57] F. Groitl, D. Graf, J. O. Birk, M. Marko, M. Bartkowiak, U. Filges, C. Niedermayer, C. Rüegg, and H. M. Rønnow, CAMEA – A novel multiplexing analyzer for neutron spectroscopy, Rev. Sci. Instr. **87**, 035109 (2016).

[58] P. Puphal, S. Allenspach, C. Rüegg, and E. Pomjakushina, Floating-Zone Growth of Sr-Substituted Han Purple: $Ba_{0.9}Sr_{0.1}CuSi_2O_6$, Crystals **9**, 273 (2019).

[59] J. Lass, H. Jacobsen, D. G. Mazzone, and K. Lefmann, MJOLNIR: A software package for multiplexing neutron spectrometers, SoftwareX **12**, 100600 (2020).

[60] C. Berthier, M. Horvatić, M.-H. Julien, H. Mayaffre, and S. Krämer, Nuclear magnetic resonance in high magnetic field: Application to condensed matter physics, Comptes Rendus Physique **18**, 331 (2017).

From surfactants to viscoelastic membranes

Gaia De Angelis and Esther Amstad
Soft Materials Laboratory, Institute of
Materials, Ecole Polytechnique Fédérale de
Lausanne (EPFL), CH-1015 Lausanne
(Switzerland)

Viviane Lutz-Bueno
Paul Scherrer Institut, Laboratory for
Neutron Scattering and Imaging,
5232 Villigen PSI (Switzerland)

Abstract

Metal coordinated bulk hydrogels gained a lot of attention in the past two decades especially due to their potential in tissue engineering, as biocompatible underwater adhesives, and self-healing substrates. Self-healing and adhesive properties would also be beneficial assets for membrane and capsule materials. Yet, such metal-coordinated hydrogels had never been used as thin membranes or even 2D films. We introduced chelator functionalized surfactants that can be ionically crosslinked at the liquid-liquid interface to form 10 nm thick viscoelastic membranes. The storage modulus and self-healing time of these membranes can be conveniently tuned with the type of chelator and crosslinking ion. Indeed, the influence of the chelator-ion pair on the storage modulus and dissipation times of thin membranes follows very similar trends to those that have been reported for corresponding metal coordinated bulk hydrogels. Hence, the vast knowhow on the composition-mechanical property relationship that exists for metal coordinated bulk hydrogels can be transferred to the behaviour of thin membranes. These insights facilitate the targeted design of viscoelastic thin membranes and capsules with appropriate storage

moduli and dissipation times which we foresee to be useful, for example, in cosmetics, drug delivery, food, or as granular inks.

I. Introduction

To protect active ingredients from harmful elements[1,2] and avoid their early contact with reagents that could lead to premature reactions or their degradation,[3,4] they are often encapsulated. Key to a successful application of capsules is a good stability and controlled permeability.[5] Capsules are frequently fabricated from emulsion drop templates. A method that offers a tight control over the dimensions of capsules is the use of double emulsions as templates. Double emulsions are small drops contained in larger drops dispersed in a third liquid. These double emulsions can be converted into capsules by solidifying their shells.[7] Unfortunately, double emulsions can only be controllably produced at low throughputs, strongly increasing the production costs of these capsules. By contrast, single emulsions, which are drops dispersed in a second liquid, can be manufactured at very high throughputs using bulk emulsification processes like vortexing[8] or sonication.[9] These drops can be converted into capsules possessing thin shells and liquid cores if they are stabilized with surfactants containing functional groups that can be covalently crosslinked.[10-13] Yet, these capsules are rather rigid and fragile, risking their breakage during manipulation and storage. Drops can also be converted into capsules possessing thin shells and liquid cores if they are stabilized with ionically crosslinkable surfactants.[14] This approach was demonstrated for emulsions that were stabilized with catechol-functionalized surfactants. However, these surfactants can only be ionically crosslinked under basic conditions.

In our work, we introduced surfactants that were functionalized with two catechol-derivatives such as pyrogallols or nitrocatechols that can complex ions also under physiologic conditions. Using Small Angle Neutron Scattering (SANS), we demonstrated that through the appropriate choice of the chelator-ion pair, we can form viscoelastic membranes as thin as 11 nm. Even though these membranes are composed of a monolayer of surfactants that are ionically crosslinked, they display storage moduli that are sufficiently high to enable their easy manipulation without compromising their integrity.[15] By comparing the rheological properties of these thin, ionically crosslinked membranes with those of corresponding metal coordinated bulk hydrogels, we demonstrated that the vast knowhow that exists on the composition-mechanical property relationship of metal coordinated hydrogels can be transferred to metal-coordinated membranes. These insights enable the targeted design of viscoelastic membranes whose storage moduli and dissipation times are appropriate, for example, for their use as water filters or in drug delivery.[16]

II. Results and discussion

A. Production of capsules

Monodisperse water-in-oil emulsion drops with diameters of 100 µm are produced with microfluidic flow focusing devices. We use water with Fe^{3+} ions at pH 9 as a dispersed

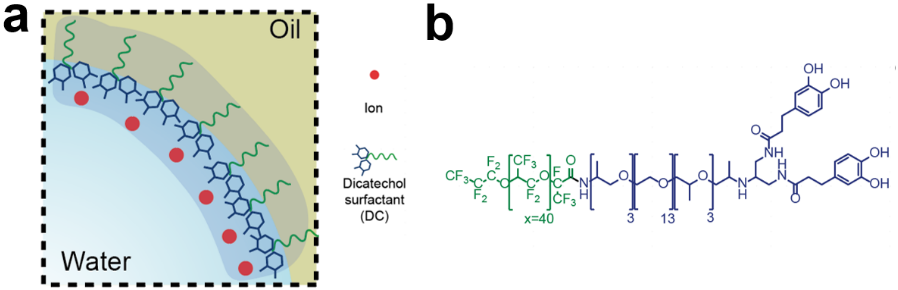

Figure 1

(a) Schematic illustration of water-in-oil emulsions stabilized with dicatechol (DC) surfactants in the presence of ions that crosslink the surfactants at the liquid-liquid interface and (b) molecular structure of DC functionalized surfactant. Adapted with permission from [15]. Copyright [2023] [Wiley-VCH GmbH].

aqueous phase and HFE7100, a perfluorinated oil, with 1 wt% surfactant as a continuous phase. We functionalize surfactants with two chelators per molecule to enable their conversion into percolating 2D films. We covalently crosslink a hydrophilic block made of an aliphatic polyether diamine derived from a propylene oxide-capped polyethylene glycol (J900) to a block-copolymer composed of a perfluoropolyether block (FSH). To enable ionic crosslinking, we couple two catechols to the two amines that are presented at the end of the hydrophilic block, as shown in Figure 1b. Upon ionic crosslinking of surfactants present at the drop surface, drops are transformed into viscoelastic capsules, as schematically indicated in Figure 1a.

B. Shell thickness part II

If surfactants form a monolayer at the liquid-liquid interface, we expect the thickness of these membranes to be in the nanometer range. Small angle scattering (SAS) is a methodology that characterizes these lengths scales of materials in bulk.[17] Small Angle Neutron Scattering (SANS) enables contrast matching between the aqueous core and the HFE7100 oil by adjusting the ratio between water (H_2O) and deuterium oxide (D_2O) in the core. If the scattering length density of the core is matched to that of the surrounding, we do not see any scattering contrast between the core and the surrounding fluid, and all the measured scattering comes from the shell.[18] The diameter of the capsules is ≈100 µm, a dimension much larger than the maximum dimension of 300 nm that we can probe with our setup (SANS-I and cSAXS). At these high magnifications, the membrane shell is observed as an infinite plane and can be modelled with a thin disk form factor P(q). The scattering intensity I(q) follows a power law decrease with q^{-2} within $0.03\ \mathrm{nm}^{-1} < q < 0.12\ \mathrm{nm}^{-1}$, as shown in Figure 2a. This result is characteristic of the Porod scattering of 2D objects. The quantitative methodology from [19] reveals a dimension of about 11 nm, a

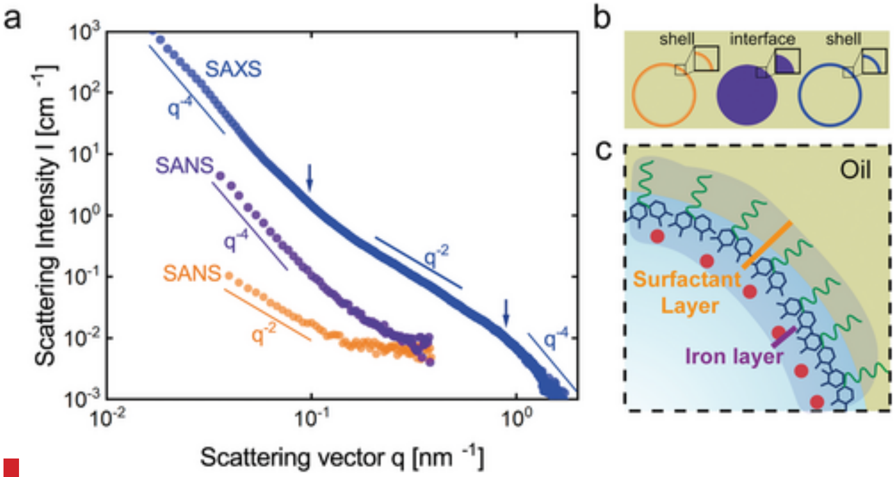

Figure 2

(a) Small angle scattering profiles of capsules produced by crosslinking the surfactant with Fe^{3+}: SANS measurements of capsules, whose contrast between the core and surrounding was matched (orange) and those with non-contrast matched aqueous cores dispersed in oil (violet). SAXS measurements of the capsules containing an aqueous core (blue). (b) Schematic illustration of the contrast and (c) schematic representation of the oil-water interface in the presence of ions and surfactants. Reprinted with permission from [15]. Copyright [2023] [Wiley-VCH GmbH].

value that agrees well with the expected shell thickness, which includes the surfactant tail, the catechol headgroups and the Fe^{3+} ions, but excludes any dimension related to the core and surrounding solvent of the capsules. To assess the surface roughness of the shells, we replace the liquid in the core with pure water to obtain a scattering contrast from the cores, as schematically shown in Figure 2b. SANS measurements reveal the scattering of a sharp interface in the same q-region, $0.03\ ^{-1} < q < 0.12\ \mathrm{nm}^{-1}$, as observed by a q^{-4} power law decay of the scattered intensity. This decay reveals a typical Porod behavior of a net flat interface and indicates that the shell interface is dense and smooth.

Neutrons strongly interact with nuclei, such that the surfactants and Fe^{3+} present in the capsule shells contribute to the observed scattering. To clearly separate contributions of the two entities, we also probe our samples using X-rays that interact with electrons. If analysed with Small Angle X-ray Scattering (SAXS), capsules have an intrinsic contrast since Fe^{3+} scatters X-rays more efficiently than the other components of the system. The scattering curve of this sample displays a power law decay of q^{-2} within $0.17\ \mathrm{nm}^{-1} < q < 0.60\ \mathrm{nm}^{-1}$, indicative of a 2D object, as shown in Figure 2a. However, compared to the SANS measurements, this decay occurs at higher q-ranges, relating to smaller dimensions.

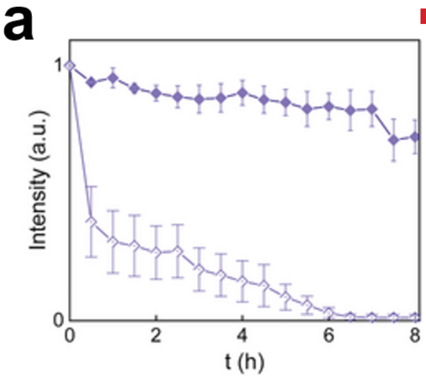

Figure 3
Fluorescent intensity of the aqueous core of capsules produced by ionically crosslinking functionalised surfactants at the drop surface. Even though the cores are composed of cell culture media, capsules effectively retain fluorescein if they are crosslinked with Fe^{3+} (◆) in contrast to their non-crosslinked counterparts (◇). Error bars represent the standard deviation of at least three repeats that have been measured on three independent samples. Adapted with permission from [15]. Copyright [2023] [Wiley-VCH GmbH].

From fitting this q-range, we calculate a dimension of about 2 nm, which could be linked to the average size of Fe^{3+} clusters that from within the tris(hydroxymethyl)aminomethane (TRIS) buffer that we employ as aqueous solution. At $q < 0.09$ nm^{-1} and $q > 0.88$ nm^{-1}, the SAXS scattering curve exhibits the decay of q^{-4}, suggesting that the Fe^{3+} aggregates also form a compact shell with a smooth interface, and that they are not dispersed in the aqueous core. Hence, scattering results reveal a total shell thickness of about 11 nm that includes an ≈2 nm thick layer that primarily contains Fe^{3+} agglomerates. Subtracting this Fe^{3+}-rich layer from the overall shell thickness of 11 nm, we find an average thickness of the shell that mainly comprises the surfactant tails of 9 nm. This value is in good agreement with the theoretical estimation of 6 nm for the fully stretched length of the perfluorinated block and 3 nm for that of the fully stretched J900 block, as calculated by adding bond lengths for the respective blocks and summarized in Figure 2c. These results support our hypothesis that the viscoelastic shell is composed of a single smooth compact monolayer of surfactants that are crosslinked with small Fe^{3+} clusters.

C. Applications

To show the potential of our capsules for drop-based high throughput screening tests and cell studies, we replace the aqueous core of the double emulsions with Dulbecco’s Modified Eagle Medium (DMEM), a cell culture media buffer. We incorporate Fe^{3+} ions into the outer phase to ionically crosslink the surfactants. To monitor the permeability of the capsules, we add 0.01 wt% of fluorescein to the core. We monitor the fluorescence of the capsule cores as a function of the incubation time in an aqueous solution. Even though the cores of these capsules are made of a cell culture media, they effectively retain encapsulants as small as 340 Da for at least 8 hours, which is the duration of our experiment. In comparison, counterparts whose shells have not been ionically crosslinked release 70% of fluorescein within 60 minutes, as shown in Figure 3a. These findings also apply to capsules produced from single

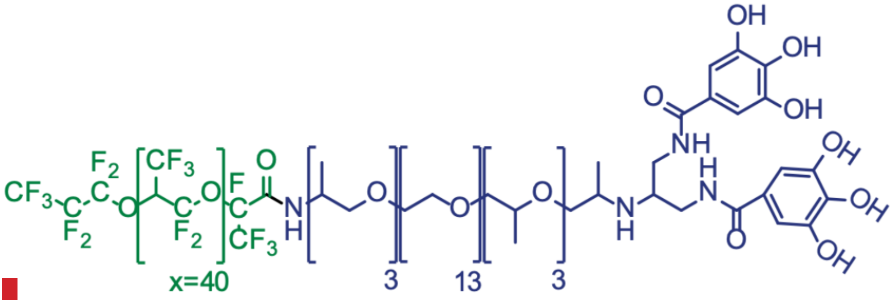

Figure 4
Molecular structure of digallol (DG) surfactant. Reprinted with permission from [15]. Copyright [2023] [Wiley-VCH GmbH].

emulsions, which can be put into aqueous solutions after ionic crosslinking of the surfactants at the drop surface without losing their integrity. These results show our capsules' potential for single-cell drop-based research and biomedical applications.

D. Expanding the toolbox of ion-chelator pairs

To broaden the range of mechanical properties of the shells of these viscoelastic capsules, we synthesise a surfactant that is functionalized with two pyrogallols per molecule, as shown in Figure 4. In contrast to catechols, which only contain two hydroxyl groups per benzene ring, pyrogallols contain a third hydroxyl group that results in lower pKa values such that these chelators can be crosslinked with divalent and trivalent ions even under physiologic conditions.[20]

E. Shell thickness part II

Surfactants and ions are expected to self-assemble into a monolayer at the liquid-liquid interface to produce a 2D film.[21,22] In the fully stretched state of surfactants, we expect the thickness of this monolayer to be around 9 nm.[15] To quantify the thickness of these pyrogallol-functionalized membranes, we performed SANS measurements on water-in-oil emulsions stabilized with this new surfactant; the drop diameters range from 10 to 50 µm. We analyse the scattering intensity *(I)* as a function of the scattering vector *(q)* to determine the shell thickness. Using the fact that the diameter of the drops is much larger than the largest length scale SANS can probe, we describe the scattering as a thin disc form factor $P(q)$.[23,24] Interestingly, the fits reveal that pure surfactants form thick shells of around 50 nm, as shown by the arrow in Figure 5a, at the q-value where the $I(q)$ slope deviates from -2. Our findings suggest that surfactants form clusters and ill-defined interfaces, as schematically depicted in Figure 5b. To assess if the ionic crosslinking increases the degree of order of surfactants at the liquid-liquid interface and thereby reduces the shell thickness, we conduct SANS experiments on shells that have been

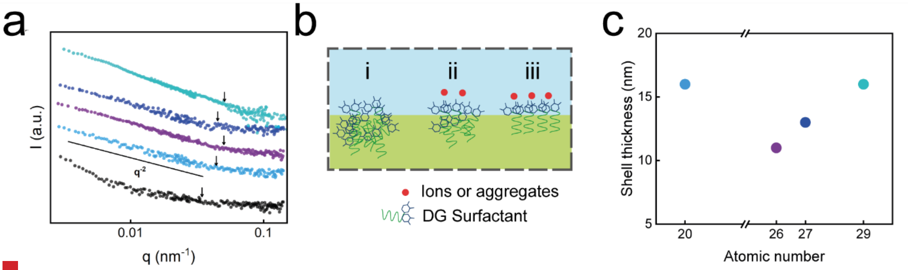

Figure 5
SANS scattering curves of emulsions whose contrast of the cores is matched to that of the surrounding phase. The emulsions are stabilized with dipyrogallol functionalized surfactants that have been crosslinked with Ca^{2+} (●), Fe^{3+} (●), Co^{2+} (●), Cu^{2+} (●) and emulsions with no ions at the interface (●). (b) Schematic illustration of the arrangement of surfactants at the water/oil interface if they are not crosslinked (i), crosslinked with weakly (ii) and strongly (iii) binding ions. (c) The shell thickness calculated from the results shown in (a) as a function of the atomic number of the crosslinking ion. Adapted with permission from [16]. Copyright [2023 American Chemical Society].

crosslinked with Ca^{2+}. Indeed, these shells exhibit a thickness of roughly 16 nm, which is noticeably thinner. Similar results are obtained when surfactants are crosslinked with other divalent ions, such as Cu^{2+}, which likewise have a low affinity for the pyrogallol molecule.[25] We crosslink them with Co^{2+} to see if we can further enhance the level of order. In fact, these shells are even thinner, 13 nm, as shown in Figure 5c. Even thinner shells with a thickness of 11 nm are obtained if surfactants are crosslinked with Fe^{3+}. This shell thickness is very similar to the predicted length of a completely stretched surfactant, which is 9 nm, indicating that these surfactants form an ionically crosslinked monolayer.[24] These results suggest that the degree of surfactant order in ionically crosslinked viscoelastic membranes and, consequently, their thickness, are determined by the affinity of the ion-chelator pair, as shown in Figure 5c.

F. A tool to compare rheological properties

To assess if the membrane stiffness, which we measure as the storage modulus, G’, correlates with the membrane thickness, we perform amplitude sweeps on flat films produced at the liquid-liquid interface using interfacial rheology. The interfacial storage (G') and loss (G'') moduli increase as the crosslinking ion's affinity for the pyrogallols increases, as shown in Figure 6a. To compare these results to their bulk counterpart, we crosslink dipyrogallol functionalized linear polyethylene glycol (PEG) with a molecular weight of 6 kDa with the same ions. We quantified their storage and loss moduli in bulk. Indeed, G' and G'' rise with increasing ion-chelator affinities in bulk hydrogels, as shown in Figure 6b and in line with the literature.[26,27] Note that the storage and loss

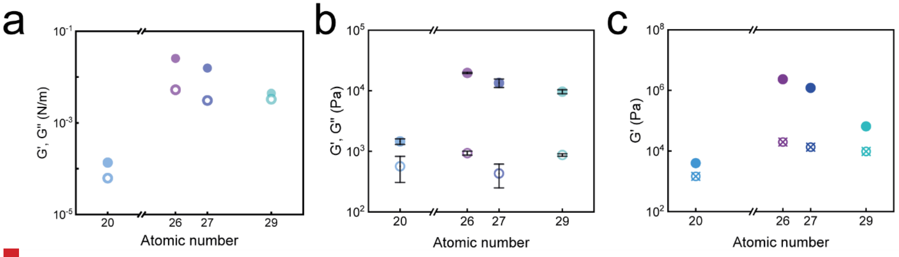

Figure 6
Storage (filled symbols) and loss (empty symbols) moduli for (a) membranes composed of surfactants and (b) 3D hydrogels composed of Di-Gallol PEG upon their crosslinking with different ions at pH 7. (c) Influence of the atomic number of the crosslinking ions on the storage moduli of viscoelastic films (filled symbols) and bulk hydrogels (empty symbols with cross). Experiments are conducted at pH 7 and the crosslinking ions are Ca^{2+} (●), Fe^{3+} (●), Co^{2+} (●) and Cu^{2+} (●). Adapted with permission from [16]. Copyright [2023 American Chemical Society].

moduli measured by bulk and interfacial rheology do not have the same dimensions, making a direct comparison impossible. To nevertheless compare these two data sets, we divide the interfacial storage moduli calculated for the membranes by their respective shell thickness and compare these values with those measured for bulk hydrogels. The trends in 2D and 3D are very similar despite the discrepancies in absolute values, as shown in Figure 6c. We attribute the discrepancies in absolute values to the differences in ionic crosslinking densities: The ionic crosslinking density in bulk hydrogels is much lower because chelators are spaced apart by a PEG 6kDa spacer. By contrast, the spacer that separates the two chelators contained in a single surfactant molecule is only a few carbons long, such that the chelator density in the thin membranes is much higher. These results indicate that we can translate the vast knowhow that exists on the influence of the chelator-ion pair on the storage, loss moduli and dissipation times of metal coordinated bulk hydrogels [28,29,30,31] to thin viscoelastic membranes. These insights strongly facilitate the targeted design of viscoelastic membranes with tuneable self-healing times, storage and loss moduli.

III. Conclusions

Surfactants functionalized with two chelators per molecule have been ionically crosslinked at the liquid-liquid interface to create well-defined viscoelastic shells that are as thin as 10 nm. The resulting capsules' stability, permeability, and self-healing properties can be finely tuned by the choice of chelator-ion pairs. Indeed, the ion-chelator dependent storage, loss moduli and dissipation times of these membranes follow similar trends as those that have been reported for corresponding metal coordinated bulk hydrogels. Hence, these parameters can be conveniently adjusted with the choice of the crosslinking ions. These findings provide new possibilities for designing self-healing, adhesive, viscoelastic membranes that can be tailored to specific needs, such as pharmaceutical and food applications.

Acknowledgments

The authors would like to thank all current and previous members of the Soft Materials Laboratory at EPFL for their vital help in getting these results, especially Francesca Bono, Chuen-Ru Li, Dr. Mathias Steinacher, Dr. Alvaro Charlet and Alexandra Thoma. They would also like to thank Dr. Enzo Bomal and Richard Blackall for their help with interfacial rheology and organic synthesis, respectively. We acknowledge the time for measurements during proposal 20210413 granted to PSI/SLS/cSAXS and proposals 20212895 and 20210940 granted to PSI/SINQ/SANS-I. We thank Ana Diaz for her support during the cSAXS beamtime, and Fabrice Cousin for the discussions about the scattering data analysis. The work was financially supported by the bioinspired materials NCCR (205603).

REFERENCES

1. X. Zhou, S. Yamashita, M. Kubota, H. Kita, *ACS Omega* 2022, 7, 5442
2. W. H. Gunzburg, M. M. Aung, P. Toa, S. Ng, E. Read, W. J. Tan, E. V. Brandtner, J. Dangerfield, B. Salmons, *Microb. Cell Fact.* 2020, 19, 216.
3. A. J. Svagan, C. B. Koch, M. S. Hedenqvist, F. Nilsson, G. Glasser, S. Baluschev, M. L. Andersen, *Carbohydr. Polym.* 2016, 136, 292.
4. M. Yan, J. Du, Z. Gu, M. Liang, Y. Hu, W. Zhang, S. Priceman, L. Wu, Z. H. Zhou, Z. Liu, T. Segura, Y. Tang, Y. Lu, *Nat. Nanotechnol.* 2010, 5, 48.
5. P. Gruner, B. Riechers, B. Semin, J. Lim, A. Johnston, K. Short, J.-C. Baret, *Nat. Commun.* 2016, 7, 10392.
6. N. Ataci, A. Sarac, *Am. J. Analyt. Chem.* 2014, 5, 22.
7. A. Vian and E. Amstad, *Soft Matter,* 2019, 15, 6, 1290-1296.
8. D. B. Flies, L. Chen, *J. Immunol. Methods* 2003, 276, 239,
9. S. Mohammad, M. Modarres-Gheisari, R. Gavagsaz-Ghoachani, M. Malaki, P. Safarpour, M. Zandi, *Ultrason. Sonochem.* 2019, 52, 88.
10. J. Du, S. P. Armes, *J. Am. Chem. Soc.* 2005, 127, 12800.
11. A. C. Bijlard, S. Winzen, K. Itoh, K. Landfester, A. Taden, *ACS Macro Lett.* 2014, 3, 1165.
12. M. Summers, J. Eastoe, R. K. Heenan, D. Steytler, J. Dispers. *Sci. Technol.* 2001, 22, 597.
13. W. Zhang, R. Wang, Z. Sun, X. Zhu, Q. Zhao, T. Zhang, A. Cholewinski, F. K. Yang, B. Zhao, R. Pinnaratip, P. K. Forooshani, B. P. Lee, *Chem. Soc. Rev.* 2020, 49, 433.
14. A. Charlet, V. Lutz-Bueno, R. Mezzenga, E. Amstad, *Nanoscale* 2021, 13, 4073.
15. G. De Angelis, N. Gray, V. Lutz-Bueno, E. Amstad, *Adv. Mater. Interfaces* 2023, 2202450
16. G. De Angelis, V. Lutz-Bueno, E. Amstad, *ACS Appl. Mater. Interfaces* 2023, 15, 19, 23758–23764
17. J. Jestin, S. Simon, L. Zupancic, L. Barre, *Langmuir* 2007, 23, 10471.
18. F. Cherhal, F. Cousin, I. Capron, *Biomacromolecules* 2016, 17, 496.
19. Cherhal, F., Cousin, F. & Capron, I. *Biomacromolecules* 17, 496–502 (2016).
20. P. Wilde, A. Mackie, F. Husband, P. Gunning, V. Morris, *Adv. Colloid Interface Sci.* 2004, 108–109, 63.
21. Seki, T. et al. *Chem* 7, 2758–2770 (2021).
22. Jensen, O. E. & Grotberg, J. B. *Phys. Fluids Fluid Dyn.* 5, 58–68 (1993).
23. Cherhal, F., Cousin, F. & Capron, I. *Biomacromolecules* 17,496–502 (2016).
24. See ref [15]

25. Ura, T. et al. *J. Chromatogr.* A 1676, 463277 (2022).
26. Bassett, D. C., Håti, A. G., Melø, T. B., Stokke, B. T. & Sikorski, P., *J. Mater. Chem.* B 4, 6175–6182 (2016).
27. Dodero, A. et al. *Eur. Polym. J.* 118, 586–594 (2019).
28. Andersen, A., Krogsgaard, M. & Birkedal, H. *Biomacromolecules* 19, 1402–1409 (2018).
29. Krogsgaard, M., Hansen, M. R. & Birkedal, H. *J Mater Chem* B 2, 8292–8297 (2014).
30. Krogsgaard, M., Behrens, M. A., Pedersen, J. S. & Birkedal, H. *Biomacromolecules* 14, 297–301 (2013).
31. Andersen, A., Chen, Y. & Birkedal, H. *Biomimetics* 4, 30 (2019).

Announcements

SGN/SNSS Members

Presently the SGN/SNSS has 197 members. New members can register online on the SGN/SNSS website: http://sgn.web.psi.ch

SGN/SSSN Annual Member Fee

The SGN/SNSS members are kindly asked to pay their annual member fees. At the general assembly 2013 of the society, the fee has been increased from CHF 10 to **CHF 20**. It can be paid either by bank transfer or in cash during your next visit at PSI. The bank account of the society is accessible for both Swiss national and international bank transfers: Postfinance: 50-70723-6 (BIC: POFICHBE), IBAN: CH39 0900 0000 5007 0723 6.

The SGN/SSSN is an organisation with tax charitable status. All fees and donations payed to the SGN/SSSN are **tax deductible**.

PSI Facility News

Recent news and scientific highlights of the three major PSI user facilities SLS, SINQ and SμS can be found in the **quarterly electronic newsletter** available online under: https://www.psi.ch/science/facility-newsletter

News from SINQ

Please visit the page https://www.psi.ch/sinq/call-for-proposals to obtain the latest information about beam cycles and the availability of the neutron instruments.

In collaboration with the Laboratoire Léon-Brillouin (Saclay, France) the instrument SANS-LLB is being commissioned at SINQ. SANS-LLB is planned to receive friendly users in the second cycle of 2023.

Registration of publications

Please remember to **register all publications either based on data taken at SINQ, SLS, SμS or having a PSI co-author** to the Digital Object Repository at PSI (DORA):
www.dora.lib4ri.ch/psi/
Follow the link 'Add Publication'.

Open Positions at SINQ and ILL

Open positions at SINQ or ILL are advertised on the following webpages:
https://www.psi.ch/pa/stellenangebote
https://www.ill.eu/careers/all-our-vacancies/?L=0

PhD positions at ILL

The PhD program of the Institut Laue-Langevin, ILL, is open to researchers in Switzerland. Consult the page https://www.ill.eu/careers/all-our-vacancies/phd-recruitment for information on the PhD program of ILL or get in contact with the managers of the program using the email address phd@ill.fr.

The Swiss agreement with the ILL includes that ILL funds and hosts one PhD student from Switzerland.

Conferences and Workshops June 2023 and beyond

An updated list with online links can be found here: http://www.psi.ch/useroffice/conference-calendar

June 2023

SNS/HFIR 2023 Neutron Scattering User Meeting
June 6-7, 2023, Oak Ridge, TN, USA

Northern Lights on Food IV
June 7-9, 2023, Lund, Sweden

BSR14: 14th International Conference on Biology and Synchrotron Radiation
June 11-14, 2023, Lund, Sweden

TNT: Training on Neutron Techniques Summer School : Inelastic Neutron Scattering
June 17-24, 2023, San Giovanni in Valle Arena (BZ), Italy

8th European Crystallography School 2023
June 18-24, 2023, Berlin, Germany

Advanced Deep Learning Train-the-Trainer
June 19-20, 2023, Dortmund, Germany

DisoMAT 2023: 2nd International School and Conference on Disorder in Materials Science
June 19-21, 2023, Plankstetten, Germany and online

FAN French neutron scattering training course
June 20-22, 2023, Grenoble, France

LightMAT 2023: 5th International Conference on Light Materials - Science and Technology
June 21-23, 2023, Trondheim, Norway and online

2023 BESSY@HZB User Meeting
June 22-23, 2023, Berlin, Germany

Gordon Research Seminar on Neutron Scattering: Realizing a Greener Future Using Neutron Techniques
June 24-25, 2023, Ventura, CA, USA

2023 Gordon Research Conference on Neutron Scattering: Neutron Scattering for a Sustainable Society
June 25-30, 2023, Ventura, CA, USA

GAMS 2023: 4th edition of the Global Advanced Materials & Surfaces
June 28-30, 2023, Paris, France

8th Edition of Nanotech France 2023
June 28-30, 2023, Paris, France

July 2023

GIREP-EPEC 2023: Physics learning promoting culture and addressing societal issues
July 3-7, 2023, Košice, Slovakia

ILL Soft Matter Summer School 2023
July 4-6, 2023, Grenoble, France

NDS 2023: 6th International Workshop on Neutron Delivery Systems
July 10-12, 2023, Grenoble, France

ICWIP2023: 8th IUPAP International Conference on Women in Physics
July 10-14, 2023, Mumbai, India

CHRNS Summer School on Methods and Applications of Neutron Spectroscopy
July 17-21, 2023, Gaithersburg, MD, USA

Gordon Research Seminar: Unconventional Experiments and Analysis Methods Enabled by Brighter X-Ray Sources
July 22-23, 2023, Easton, MA, USA

Gordon Research Conference: Observing Complex Systems in Space and Time with Tailormade X-Rays from Next-Generation Sources
July 23-28, 2023, Easton, MA, USA

ICCGE-20: International Conference on Crystal Growth and Epitaxy
July 30 - August 7, 2023, Naples, Italy

EBSA Congress 2023
July 31 - August 4, 2023, Stockholm, Sweden

August 2023

25th National School on Neutron and X-ray Scattering
August 6-8, 2023, Argonne (IL) and Oak Ridge (TN), USA

Deep Learning School Basic Concepts
August 19-20, 2023, Dortmund, Germany

RÅC International Summer School: Cutting-edge Neutron and X-ray Research for a Sustainable Future
August 20-27, 2023, Lüneburg, Germany

IUCr 2023: 26th Congress and General Assembly of the International Union of Crystallography
August 22-29, 2023, Melbourne, Australia

Polarised Neutrons - Future Directions: microsymposium at IUCr 2023
August 22-29, 2023, Melbourne, Australia

Methods for the Determination and Analysis of Magnetic Structures: microsymposium at IUCr 2023
August 22-29, 2023, Melbourne, Australia

X-ray ptychography: microsymposium at IUCr 2023
August 23, 2023, Melbourne, Australia

FLS 2023: 67th ICFA Advanced Beam Dynamics Workshop on Future Light Sources
August 27 - September 1, 2023, Lucerne, Switzerland

ESERA 2023: 15th Conference of the European Science Education Research Association
August 28 - September 1, 2023, Cappadocia, Turkey

September 2023

FEMS EUROMAT 2023
September 3-7, 2023, Frankfurt a.M., Germany and online

ECIS 2023: 37th Conference of the European Colloid and Interface Society
September 3-8, 2023, Naples, Italy

International Summer Programme on Neutron and X-Ray Science for undergraduate students
September 3-29, 2023, Grenoble, France

2nd Women in Physics Career Symposium
September 4, 2023, Basel, Switzerland

SPS Annual Meeting 2023 (with special topical session on neutron science)
September 4-8, 2023, Basel, Switzerland

25th JCNS Laboratory Course Neutron Scattering
September 4-15, 2023, Jülich and Garching, Germany

PSI Synchrotron Powder Diffraction School 2023
September 11-15, 2023, Villigen, Switzerland

SXR2023 – Principles of Functionality from Soft X-ray Spectroscopy
September 11-15, 2023, Berlin, Germany

Advanced Deep Learning Active Training Course
September 25-29, 2023, Meinerzhagen, Germany

October 2023

Trends and Perspectives in Neutron Scattering: Future Instruments at Pulsed Sources
October 9-12, 2023, Tutzing, Germany

UCANS: 10th annual meeting of the Union for Compact Accelerator-driven Neutron Sources
October 16-19, 2023, Budapest, Hungary

EGF 2023: 8th Edition of the European Graphene Forum
October 25-27, 2023, Albufeira-Algarve, Portugal

8th edition of the Smart Materials and Surfaces International Conference
October 25-27, 2023, Albufeira-Algarve, Portugal

SiMol: Simulation Meets Molecular Spectroscopy Meeting
October 30 - November 1, 2023, Abingdon, UK

November 2023

SR2A 2023: 10th International Conference on Synchrotron Radiation and Neutrons in Art and Archaeology
November 21-24, 2023, Munich, Germany

December 2023

MRM2023: Advanced Materials Research Grand Meeting 2023
December 11-16, 2023, Kyoto, Japan

HIRES 2023: Synergies in HIgh RESolution Spectroscopy
December 12-15, 2023, Grenoble, France

Minutes of the SGN/SSSN/SNSS General Assembly 2022

Date/Location
December 2, 2022,
Virtual meeting via Zoom

Start
15:00

End
16:30

Participants
29 members of the society and
5 non-members

1. Welcome

Marc Janoschek, president of the Swiss Neutron Science Society, welcomes the participants to the general assembly 2022.

2. Minutes of the General Assembly 2021

The minutes of the general assembly of the SNSS/SGN from 26.11.2021, published in Swiss Neutron News #59 are accepted by all 23 members present at the assembly.

3. Annual Report of the Chairman

Marc Janoschek reports on the activities of the SNSS/SGN in the years 2021 and 2022:

a. The SNSS has organized and participated in several workshops and symposiums. At the SPS meeting held in June 2022, the SNSS has organized the symposium “Swiss Neutron Science on the European Scale”. The poster prizes at the Swiss Soft Day 29 (April 2022) and the French-Swiss Meeting “SANS for Soft Matter” held in Strasbourg (March 2022) were sponsored by the SNSS.

b. The ninth (2022) **Young Scientist Prize** of the SNSS/SGN sponsored by Swiss Neutronics has been awarded to **Dr. Stephan Allenspach** (UniGE). Nominations for the 2023 Young Scientist Prize of the SNSS should be submitted to the Swiss Neutron Science Society (sgn@psi.ch) until March 5, 2023.
c. Several outstanding Swiss contributions to neutron science have been honored with awards: The European Neutron Association (ENSA) awarded **Dr. Ellen Fogh** (EPFL) the Felix Lewy Bertaud Prize. The Swiss scientist **Prof. Peter Böni** (Technical University Munich) was awarded the Walter Hälg Prize by ENSA. **Dr. Artur Glavic** (PSI) received the inaugural Instrumentation Prize of the German "Committee Research with Neutrons (KFN)".
d. The SNSS/SGN has **198 members** at the time of the assembly. There are many more profiting from neutron science in Switzerland, and a mechanism to include them in SNSS would be very welcome. In the years from 2015 to 2020, there were 419 unique proposers with email addresses ending with ".ch" submitting research proposals to SINQ. In the same time range, there were more than 500 publications including an author with Swiss affiliation.
e. Two issues of Swiss Neutron News have appeared in May 2022 and at the end of November 2022..

4. Report of the Treasurer

The annual balance sheet for 2021 is presented:

Assets SNSS/SGN on 1.1.2021:	**CHF 8161.80**

	Revenues [CHF]	**Expenses [CHF]**
Membership-fees (cash box)	0.00	
Membership-fees (postal check acc.)	615.00	
Donations	30.00	
Deposit prize money 2021	1000.00	
Expenses Postfinance account		64.00
Payout prize money 2021		1000.00
Total	1645.00	1064.00
Net earnings 2021	**581.00**	

Balance sheet 2021:	**Assets [CHF]**	**Liabilities [CHF]**
Postfinance account	8522.80	
Cash box	220.00	
Assets on 31.12.2021	**8742.80**	

5. Report of the Auditors

Both Auditors (Dr. M. Zolliker and Prof. F. Piegsa) have examined the bookkeeping and the balance sheet for 2021. They have accepted it without objection. The participants unanimously vote for the release of the SGN/SNSS board.

1.2.22
Datum
Dr. M. Zolliker, PSI

11.2.22
Datum
Prof. Florian Piegsa, Univ. Bern

6. Vote for a new Auditor

Prof. Florian Piegsa is a board member of SNSS since 2022 and, therefore, cannot continue to act as an Auditor. Dr. Daniel Mazzone (PSI) has kindly agreed to take on this role. Daniel Mazzone is unanimously confirmed as new Auditor of SNSS.

7. Budget 2023

Marc Janoschek presents the following proposal for the budget 2023:

	Receipts [CHF]	**Expenditures [CHF]**
member fees	700.00	
interest	0.00	
prize money	1000.00	1000.00
fees Postfinance account		63.00
Financing of poster awards etc.		500.00
Total	1700.00	1563.00
Total receipts 2023	137.00	
Assets 31.12.2023	9409.18	

The participants accept the budget proposal without objection.

8. Proposal / Decision to Change Membership Model

The Swiss Neutron Science Society (SNSS) currently has about 200 members, but only a small fraction are paying members. The society has never enforced payment because the income was sufficient. In addition, we currently benefit from PSI graciously covering the cost for printing Swiss Neutron News and to host the website. However, the website system is outdated and will eventually be retired. If SINQ users would automatically become members of the society, the SNSS could have 500+ members, but younger and new neutron scientists often do not join. To address this, the society is proposing an additional Institutional Membership model, where institutions such as PSI or university groups can pay for their staff to be members. This would stabilize the society's income and allow for additional measures such as student travel grants and organization of topical workshops.

This proposal is connected with the proposal to make SNSS a member organization of SCNAT described below.

9. SCNAT Membership

Research societies can become member societies of SCNAT, which has many benefits such as having their webpages hosted on SCNAT platform and being able to apply for additional funds for various purposes such as summer schools/workshops, travel funds for members, and education measures. In addition, SCNAT has an excellent relationship with the State Secretariat for Education, Research and Innovation (SERI), which is the national funding body funding PSI, many of the Swiss large-scale facility projects, and the access to international neutron sources such as the ILL and ESS. SCNAT is also leading the national roadmap process. Thus, being part of SCNAT would also enable event better exchange with SERI and other scientific societies that have common goals and interests (such as CHIPP, SPS, SGK/SSCr).

However, there is a cost of 7 CHF/member/year, which adds up to about 1500 CHF/year for SNSS. Despite this, once the initial investment is made, a multiple of it can be recovered.

The board proposes that SNSS joins SCNAT. The SCNAT membership and the change of the membership model (paragraph 8) are adopted with 25 votes in favour, none against and 4 abstentions.

10. News from ENSA, ILL, and ESS

I) **News from SINQ** (Michel Kenzelmann)

a. The call for SINQ proposals of Nov. 15, 2022, was very successful with 325 proposals for 12 instruments. This is about 7% more than for the call of May 15, and it reflects the high demand for beam time at SINQ, because other neutron sources have been shut down or not in operation.

b. SINQ/PSI is a partner of the European project ReMade@ARI, which was accepted. This project forms a consortium of world-class research infrastructures for materials characterization in a circular economy.

c. Two new/upgraded instruments at SINQ have joined user operation: The multiplexing spectrometer CAMEA is optimized for small samples and complex sample environments. It can compete with flag-ship spectrometers at ILL or NIST. Together with MLZ, the diffractometer DMC was rebuilt with a much larger detector.

d. The upgrades of four SINQ instruments are continued: The reflectometer AMOR and the small-angle instrument SANS-LLB are planned to join user operation in the second cycle of 2023. The imaging beam line NEUTRA is upgraded for higher flux and higher resolution. The materials-science diffractometer POLDI is upgraded to increase ists performance for engineering diffraction by a factor of 5.
e. ANAXAM is now an established and successful public-private partnership catering to industrial needs at large facilities, with an increasing number of industry-related projects at SINQ using more than 40 beam days per year.
f. A project for a Neutron Guide Hall North for about 6 additional instruments at SINQ is being discussed. This would be a quite inexpensive way to increase the amount of neutron beam time available in Europe. This project may be realized after 2030 and a preliminary report is planned for 2025.
g. Instead of a user meeting, several focused workshops have been organized by scientists at SINQ: the French-Swiss workshop on SANS for Soft Matter, the workshop Topology in Magnetic Materials, the workshop on Nordic Perspectives on Advanced Neutron Imaging, the Zuoz-PSI Condensed Matter Camp on Coherence and Entanglement in Quantum Systems, and the workshop on Perspectives with High Magnetic Fields at Neutron Sources.
h. Prizes awarded in 2022 to scientists affiliated the Laboratory for Neutron Scattering and Imaging and the Laboratory for Neutron and Muon Instrumentation: Dr. Alessandra Luchini (ESS, PSI) was awarded the Camurus Lipid Research Foundation Junior Prize. Dr. Arthur Glavic (PSI) received the KFN Instrumentation Prize.

II) **News from ENSA** (Henrik Rønnow)

a. ENSA is chaired by Henrik Rønnow (EPFL Lausanne), the vice chair is Lambert van Eijck (TU Delft), and the secretary is Natalie Malikova (Sorbonne Université, Paris). The Swiss delegate to ENSA is Marc Janoschek (PSI).
b. The European Neutron conference ECNS, co-organized by ENSA, will take place in March 2023 in Munich.
c. ENSA has published three calls for prizes: the Walter Hälg Prize for outstanding efforts and achievements in neutron scattering, the Levy Bertaut Prize for notable experimental, methodological or theoretical contributions to the investigation of matter using crystallographic or neutron scattering methods, and the Neutron Instrumentation and Innovation Award.
d. ENSA has issued a call for the International Conference on Neutron Scattering (ICNS) 2025. The deadline is January 25, 2023.
e. Currently ENSA is discussing its position with regard to our Russian colleagues from the Russian Neutron Scattering Society (ROSNEUTRO). This was triggered by ECNS having to formally exclude Russian scientists because of German sanctions due to Russia’s war of aggression in Ukraine.
f. ENSA is attempting to establish collaborations with other organizations for Transnati-

onal Access (TNA) to neutron sources. Discussions are held with ESUO, LENS, and LEAPS.

III) **News from ILL** (Marc Janoschek)

a. A contract for the Swiss 2019-2023 membership in ILL has been signed, with thanks to SERI. Contract negotiations for the next period will start in early March 2023.

b. Funding for the Swiss membership has been secured in SERI Botschaft until 2028. SERI is considering negotiating a contract that will go up to at least 2028.

c. Initially, the Swiss contribution to ILL was expected to decrease from 15 MCHF to 12 MCHF due to investment in ESS, but SERI is considering using 3-4 MCHF from credit for ESS to stabilize or even slightly increase the contribution to ILL.

d. The Swiss-CEA-CRG collaboration gives beamtime on IN22, IN12, and D23 through the normal ILL proposal system. The contract is valid through 2023, and negotiations are underway to extend it up to 2027.

e. The PSI-ILL collaborations have added synergies, such as high-pressure and soft matter sample environments. This collaboration is continued, and a recent PSI-ILL meeting discussed expanding the PSI-ILL bilateral collaboration.

f. ILL has not been able to run full annual schedules in recent years. Researchers whose work is impeded by national balance should send a message to document the science not done or postponed.

IV) **News from ESS** (Marc Janoschek)

a. The outside construction and the office buildings of ESS are finished. Good progress was also made with the accelerator, which is mostly on time.

b. The PSI-ESS project and its partners are making good progress with installations at ESS for BIFROST (CAMEA-like spectrometer), ESTIA (reflectometer with Selene guides), and the multi-purpose imaging instrument ODIN. It is expected that these installations will be ready for first Beam On Target (BOT).

c. However, the overall ESS project continues to experience delays, with the current projection for BOT in January 2026. The most critical issue is the He gas circulator for the target.

11. Miscellaneous

A question is asked about the He situation at the PSI. Marc Janoschek informs that the availability of He is as yet not a big problem thanks to the good recovery system. For some Swiss Universities, He supply has become a significant problem.

U. Gasser
February 2023

Editorial

Editor
Dr. V. Lutz-Bueno
Viviane.lutz-bueno@psi.ch

Board for the Period 2022 – 2024:
President
Prof. Dr. M. Janoschek
marc.janoschek@psi.ch

Board Members
PD Dr. U. Gasser
urs.gasser@psi.ch

PD Dr. K. Krämer
karl.kraemer@dcb.unibe.ch

Prof. Dr. F. Piegsa
florian.piegsa@lhep.unibe.ch

Prof. Dr. H. Rønnow
henrik.ronnow@epfl.ch

Prof. Dr. M. Strobl
markus.strobl@psi.ch

Honorary Members
Prof. Dr. W. Hälg, ETH Zürich (†)

Prof. Dr. K. A. Müller
IBM Rüschlikon and Univ. Zürich

Prof. Dr. A. Furrer
ETH Zürich and Paul Scherrer Institut

Auditors
Dr. M. Zolliker, Paul Scherrer Institut
Prof. Dr. F. Piegsa, Univ. Bern

Address
Sekretariat SGN/SSSN/SNSS
c/o Paul Scherrer Institut
WLGA/018
CH-5232 Villigen PSI
phone: +41 56 310 46 66
fax: +41 56 310 32 94
http://sgn.web.psi.ch

Bank Account
Postfinance: 50-70723-6 (BIC: POFICHBE)
IBAN: CH39 0900 0000 5007 0723 6

Printing
Paul Scherrer Institut
Circulation: 1600
2 numbers per year

Swiss Neutron Science Society
Sekretariat SGN/SSSN/SNSS
WLGA/018
Paul Scherrer Institut
5232 Villigen PSI, Switzerland

Join the Swiss Neutron Science Society...

to support all science using neutron radiation in Switzerland.
The Swiss Neutron Science Society is open to everybody interested in neutron scattering and research using neutron radiation in general.

The annual membership fee is CHF 20.-, but the membership is free for Bachelor-, Master-, and PhD-students.

Send an email to sgn@psi.ch to join.